2018 European Control Conference (ECC)
June 12-15, 2018. Limassol, Cyprus

Higher order sliding mode and adaptive backstepping controllers for a full-car model with active suspension*

Juan J. Ley-Rosas[1], Jorge E. Ruiz-Duarte[1], Luis E. González-Jiménez[2] and Alexander G. Loukianov[1].

Abstract— **The robust stabilization of the vertical position, pitch and roll dynamics of the center of gravity for a vehicle with active suspension is addressed in this work. Three different higher order sliding mode (HOSM) control algorithms and an adaptive backstepping controller (ABC) are designed to fulfill the control objective. First, two second order sliding mode controllers, the quasi-continuous and the nested, are designed to stabilize the 2-relative degree vertical position. Then, a super-twisting (ST) algorithm is designed, by means of a 1-relative degree sliding function, obtaining asymptotic stability. For the ABC, adaptive parameters dynamics are proposed, as well as the control law that adds desired linear dynamics. Finally, a performance comparison between the proposed controllers is presented based on simulations results.**

I. Introduction

The suspension systems for automobiles play an important role in modern vehicles because they provide comfort and stability in driving. Their functions are: to isolate the chassis of the road irregularities, to reduce the force transmitted to the driver, and to control the vertical movement of the tires. Also, these systems permit to ensure contact between the tires and the road in order to maintain the maneuverability and to prevent damage of the vehicle while driving on irregular terrains. A simple suspension can be modeled only with a spring and damper, this kind of suspension is known as passive suspension. Exist other two types of suspensions known as semi-active and active suspension. The first one does not include actuators, but is characterized by having adjustable dampers [1]. The second one is more complex because it incorporates sensors, actuators and controllers. At a functional level, the most easily appreciated feature of this system is that each wheel has independent control, which makes the active suspension an excellent system for gaining greater stability, safety and adhesion to the road; making it a system significantly superior to the passive suspension. For these reasons, there are many works, i.e., [2], [3] which use active suspension for comfort of the passenger, which depends on a combination of vertical and angular motion (pitch and roll) for stability. Besides, there exist three models to represent the suspension system: quarter-car model, half-car model and full-car model. Quarter-car model is a 2 degrees-of-freedom (DOF) system and represents the suspension system at any of the four wheels of the vehicle. The degrees-of-freedom are displacement of axle and displacement of the vehicle body at the particular wheel. On the other hand, half-car model is a 4 DOF system and represents vertical displacement, vertical velocity, pitch angular displacement and pitch angular velocity. To end, the full-car model has 7 DOF which represent the vertical position, the pitch and roll angles of the vehicle body and the vertical motions of each of the four unsprung masses. Due to the mentioned above, the combination of using an active suspension, considering the full-car model which provides a more precise representation of the system, and the well known robustness of a sliding mode (SM) controller results in the improvement of passenger comfort and vehicle stability. In this work, three different SM algorithms and an ABC are proposed for the stabilization of the vertical position, pitch and roll motions of a car, considering a full-car model with active suspension. The paper is organized as follows. The dynamic model of active suspension with full car model is presented in section II. Controllers design is shown in Section III. In section IV, the performance of the proposed controllers is presented via simulation results. Finally, in section V, the conclusions of the work are outlined.

*This work was supported by CONACYT, Mexico, under grant 252405.

[1]Juan J. Ley-Rosas, Jorge E. Ruiz-Duarte and Alexander G. Loukianov are with the Automatic Control Laboratory, Cinvestav Guadalajara, 45019, Zapopan, Jalisco, Mexico. {jley,jeruiz,louk}@gdl.cinvestav.mx

[2]Luis Enrique González-Jiménez is with Department of Electronics, Systems and Computing, ITESO AC, 45604, Tlaquepaque, Jalisco, Mexico. luisgonzalez@iteso.mx

II. Dynamic model of active suspension with full car model

A full car model (7-DOF) [4] is used in this work. The sprung mass dynamics of the i-th suspension is defined as

$$\ddot{x}_{1,i} = \frac{1}{m_{s,i}}(-f_{s,i} + u_i), \tag{1}$$

while the unsprung mass dynamics is given by

$$\ddot{x}_{3,i} = \frac{1}{m_{u,i}}(f_{s,i} - f_{t,i} + u_i), \tag{2}$$

where $i = RL, RR, FL, FR$ is rear left, rear right, front left or front right locations of the wheels, u_i is the corresponding control input, and $m_{s,i}$ and $x_{1,i}$ are the mass and position of the sprung mass of each suspension, respectively. The terms $m_{u,i}$ and $x_{3,i}$ are the mass and position of the unsprung mass of each suspension, respectively. The road disturbance for the i-th wheel is given by $z_{r,i}$, the different suspension forces $f_{s,i}$ of (1) and (2) are given by

$$f_{s,i} = K_i(x_{1,i} - x_{3,i}) + B_i(x_{2,i} - x_{4,i}) \tag{3}$$

and tire forces are

$$f_{t,i} = K_{t,i}(x_{3,i} - z_{r,i}) + B_{t,i}(x_{4,i} - \dot{z}_{r,i}) \tag{4}$$

where K_i and B_i are the suspension spring stiffness coefficients and the suspension damping coefficients, and $K_{t,i}$ and $B_{t,i}$ are the tire stiffness parameters and tire damping, $x_{2,i}$ and $x_{4,i}$ are the velocities of the sprung mass and the unsprung mass of the each suspension, respectively.
The second order model for each subsystem of (1) is

$$\begin{aligned}\dot{x}_{1,i} &= x_{2,i}\\ \dot{x}_{2,i} &= \frac{1}{m_{s,i}}[-K_i(x_{1,i}-x_{3,i})-B_i(x_{2,i}-x_{4,i})+u_i].\end{aligned} \tag{5}$$

With (3) and (4), (2) becomes

$$\begin{aligned}\ddot{x}_{3,i} &= \frac{1}{m_{u,i}}[K_i(x_{1,i}-x_{3,i})+B_i(x_{2,i}-x_{4,i})\\ &- K_{t,i}(x_{3,i}-z_{r,i})-B_{t,i}(x_{4,i}-\dot{z}_{r,i})+u_i].\end{aligned} \tag{6}$$

Terms $x_{3,i}$ and $x_{4,i}$ will be considered as disturbances for the dynamics systems defined by (5). The roll motion of the sprung mass of the car is described by the following equation

$$\begin{aligned}\ddot{\theta} &= \frac{1}{I_x}\big[(f_{s,RL}+f_{s,FL}-u_{RL}-u_{FL})d\\ &\quad -(f_{s,RR}+f_{s,FR}-u_{RR}-u_{FR})d\big],\end{aligned} \tag{7}$$

while the pitch motion of the sprung mass of the car can be expressed as

$$\begin{aligned}\ddot{\phi} &= \frac{1}{I_y}\big[(f_{s,FL}+f_{s,FR}-u_{FL}-u_{FR})a\\ &\quad -(f_{s,RL}+f_{s,RR}-u_{RL}-u_{RR})b\big],\end{aligned} \tag{8}$$

and the vertical motion of the sprung mass of the car is

$$\begin{aligned}\ddot{z}_1 &= -\frac{1}{M_s}\big(f_{s,RL}+f_{s,RR}+f_{s,FL}+f_{s,FR}\\ &\quad -u_{RL}-u_{RR}-u_{FL}-u_{FR}\big),\end{aligned} \tag{9}$$

where I_x is the moment of the inertia at roll axis, I_y is the moment of the inertia at pitch axis, M_s is the total mass of the automobile, a is the distance between the center of gravity (C.G.) and the front wheels, b is the distance between the C.G. and the rear wheels, and $2d$ is the automobile width. Finally, the car model considered in this work is defined by equations (5), (6), (7), (8) and (9).

III. Controllers design

The control objective is to keep $x_{1,i}$ as close to zero as possible, rejecting the effect of $x_{3,i}$ in system (5). This to maintain the safety and comfort of the passenger. Accordingly, in this section, three sliding mode control algorithms are proposed to stabilize the vertical position (z_1), pitch (ϕ) and roll (θ) motions at the car center of gravity despite road disturbances at each wheel.

A. Quasi-continuous and nested-sliding mode controllers

Let $x_{1,i}$ be the output variable of an uncertain single input-single-output dynamic system. The task is to establish the sliding functions $\sigma_i = x_{1,i}$ as low as possible. The standard SM control $u_i = -k\text{sign}(\sigma_i)$ is applicable, if the output relative degree is 1, i.e., if $\dot{\sigma}_i$ explicitly depends on the control u_i. The corresponding finite-time convergent controllers (r-sliding controllers) require only the knowledge

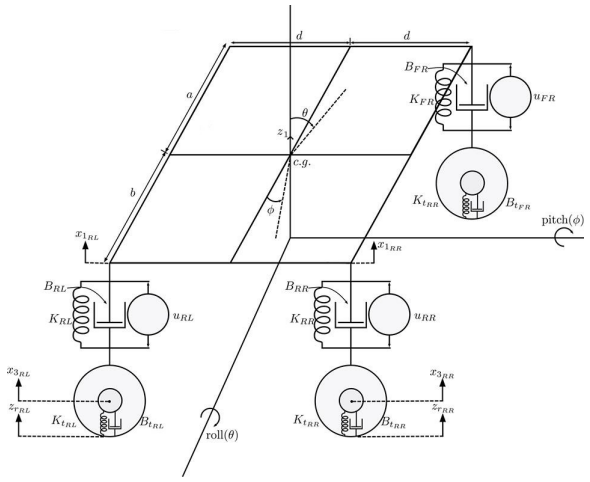

Fig. 1. Diagram for the full car model

of the systems relative degree r, in this case $r = 2$. The produced control is a discontinuous function of σ_i and $\dot{\sigma}_i$. The homogeneous quasi-continuous controller and the nested-sliding-mode-controller proposed in [5] are used in this work. In both controllers, the produced control law is a function of the state variables, which is continuous everywhere except the r-sliding set:

$$\sigma_i = \dot{\sigma}_i = 0. \tag{10}$$

For both controllers, the control law can be represented by

$$u_i = -\alpha\Psi_i \tag{11}$$

where α is a positive constant. If quasi-continuous controller is applied, Ψ_i is defined by

$$\Psi_i = \frac{\dot{\sigma}_i + \big|\sigma_i\big|^{1/2}\text{sign}(\sigma_i)}{\big|\dot{\sigma}_i\big| + \big|\sigma_i\big|^{1/2}}, \tag{12}$$

and for nested-sliding-mode controller, Ψ_i is defined by

$$\Psi_i = \text{sign}[\dot{\sigma}_i + \big|\sigma_i\big|^{1/2}\text{sign}(\sigma_i)]. \tag{13}$$

In order to implement (12) or (13), it is necessary to know the time derivative of the sliding vector σ_i. For that purpose, a second-order robust exact differentiator [5] is used for the estimation of $\dot{\sigma}_i$ which is defined as follows:

$$\begin{aligned}\dot{\zeta}_0 &= -\lambda_2 L^{1/3}\big|\zeta_0-\sigma_i\big|^{2/3}\text{sign}(\zeta_0-\sigma_i)+\zeta_1\\ \dot{\zeta}_1 &= -\lambda_1 L^{2/3}\big|\zeta_0-\sigma_i\big|^{1/3}\text{sign}(\zeta_0-\sigma_i)+\zeta_2\\ \dot{\zeta}_2 &= -\lambda_0 L\text{sign}(\zeta_0-\sigma_i),\end{aligned} \tag{14}$$

where ζ_0, ζ_1 and ζ_2 are the estimates of σ_i, $\dot{\sigma}_i$ and $\ddot{\sigma}_i$, respectively. The parameters λ_1, λ_2, λ_3 and L are the gains of the differentiator and permit to define its convergence time.

B. Super-Twisting Control

The design procedure for this controller is proposed as follows: the four sliding functions are designed as

$$\sigma_i = C_i x_{1,i} + x_{2,i}, \tag{15}$$

where C_i are design constants. The sliding functions dynamics are described by

$$\dot{\sigma}_i = C_i x_{2,i} + \frac{1}{m_{s,i}}(-f_{s,i} + u_i). \tag{16}$$

From (15) and (3), (16) is given by

$$\dot{\sigma}_i = \Delta_{1,i} + \Delta_{2,i} + \frac{1}{m_{s,i}} u_i, \tag{17}$$

with

$$\begin{aligned} \Delta_{1,i} &= (C_i - \frac{B_i}{m_{s,i}})\sigma_i, \\ \Delta_{2,i} &= (C_i \frac{B_i}{m_{s,i}} - C_i^2 - \frac{K_i}{m_{s,i}})x_{1,i} \\ &+ \frac{1}{m_{s,i}}(K_i x_{3,i} + B_i x_{4,i}). \end{aligned} \tag{18}$$

A control law must be designed such that the sliding functions σ_i achieves the sliding surface

$$\Sigma_i := \left\{ x_{1,i}, x_{2,i} \mid \sigma_i = 0 \right\}$$

in finite time. The SM control is proposed by using the ST algorithm [6] of the form

$$\begin{aligned} u_i &= m_{s,i}[-k_{1,i}|\sigma_i|^{1/2}\text{sign}(\sigma_i) + v_i] \\ \dot{v}_i &= -k_{2,i}\text{sign}(\sigma_i), \end{aligned} \tag{19}$$

where $k_{1,i}$ and $k_{2,i}$ are positive constants. The closed-loop system (17)-(19) results in

$$\begin{aligned} \dot{\sigma}_i &= -k_{1,i}|\sigma_i|^{1/2}\text{sign}(\sigma_i) + v_i + \Delta_{1,i} + \Delta_{2,i} \\ \dot{v}_i &= -k_{2,i}\text{sign}(\sigma_i). \end{aligned} \tag{20}$$

The system (20) stability can be demonstrated as in [7]. The perturbation $\Delta_{2,i}$ is non-vanishing with respect to σ_i. Then, it is necessary to perform a transformation of the form

$$\varsigma_i = v_i + \Delta_{2,i}. \tag{21}$$

System (20) becomes

$$\begin{aligned} \dot{\sigma}_i &= -k_{1,i}|\sigma_i|^{1/2} sign(\sigma_i) + \varsigma_i + \Delta_{1,i} \\ \dot{\varsigma}_i &= -k_{2,i} sign(\sigma_i) + \dot{\Delta}_{2,i}. \end{aligned} \tag{22}$$

Therefore, there exists a finite time such that Σ_i is achieved by system (5) with

$$\begin{aligned} k_{1,i} &> 2\delta_{1,i}; \\ k_{2,i} &> k_{1,i}\frac{5\delta_{1,i}k_{1,i} + 6\delta_{2,i} + 4(\delta_{1,i} + \delta_{2,i}/k_{1,i})^2}{2(k_{1,i} - 2\delta_{1,i})}; \end{aligned} \tag{23}$$

under the assumptions

$$|\Delta_{1,i}| \leq \delta_{1,i}|\sigma_i|^{1/2}, \qquad |\dot{\Delta}_{2,i}| \leq \delta_{2,i}. \tag{24}$$

for some constants $\delta_{1,i} \geq 0$ and $\delta_{2,i} \geq 0$.
When sliding motion is reached, the controller (19) forces the system (16) to remain in the manifold $\sigma_i = 0$, and as a consequence $x_{2,i} = -C_i x_{1,i}$. Using the variables $x_{2,i}$ as pseudo-controllers for the $x_{1,i}$ dynamics results in

$$\dot{x}_{1,i} = -C_i x_{1,i}, \tag{25}$$

which is a globally exponentially stable system.

As well as the road disturbance increases, the bound of $f_{s,i}$ will increase too. Then, the ST gains must be chosen such that passenger comfort is achieved and considering the physical actuators limitations.

C. Adaptive backstepping control

For the design of the controller by ABC [8], the model (5) can be rewritten according to the parameters to be adapted,

$$\begin{aligned} \dot{x}_{1,i} &= x_{2,i} \\ \dot{x}_{2,i} &= -\theta_{1,i}(x_{1,i} - x_{3,i}) - \theta_{2,i}(x_{2,i} - x_{4,i}) + \theta_{3,i}u_i, \end{aligned} \tag{26}$$

where

$$\theta_{1,i} = \frac{K_i}{m_{s,i}}, \quad \theta_{2,i} = \frac{B_i}{m_{s,i}}, \quad \theta_{3,i} = \frac{1}{m_{s,i}}. \tag{27}$$

The error variable is defined as

$$\sigma_{1,i} = x_{1,i} - y_{r,i}, \tag{28}$$

where $y_{r,i}$ is the desired position. In this case $y_{r,i} = 0$. The derivative w.r.t time is

$$\dot{\sigma}_{1,i} = \dot{x}_{1,i} = x_{2,i}. \tag{29}$$

The Lyapunov function for $\sigma_{1,i}$ can be defined as

$$V_{1,i} = \frac{1}{2}\sigma_{1,i}^2, \tag{30}$$

differentiating $V_{1,i}$ w.r.t time,

$$\dot{V}_{1,i} = \sigma_{1,i}\dot{\sigma}_{1,i} = \sigma_{1,i}x_{2,i}. \tag{31}$$

From (31), the desired variable can be expressed as

$$x_{2d,i} = -k_{1,i}\sigma_{1,i}, \tag{32}$$

the second error variable is defined as:

$$\sigma_{2,i} = x_{2,i} - x_{2d,i} \tag{33}$$

hence

$$x_{2,i} = \sigma_{2,i} - k_{1,i}\sigma_{1,i} \tag{34}$$

and from (31) and (34)

$$\dot{V}_{1,i} = \sigma_{1,i}(\sigma_{2,i} - k_{1,i}\sigma_{1,i}) = \sigma_{1,i}\sigma_{2,i} - k_{1,i}\sigma_{1,i}^2. \tag{35}$$

Derivating (33)

$$\begin{aligned} \dot{\sigma}_{2,i} &= \dot{x}_{2,i} - \dot{x}_{2d,i} = -\theta_{1,i}(x_{1,i} - x_{3,i}) \\ &- \theta_{2,i}(x_{2,i} - x_{4,i}) + \theta_{3,i}u_i + k_{1,i}\dot{\sigma}_{1,i}. \end{aligned} \tag{36}$$

Lyapunov function $V_{2,i}$ is defined by

$$V_{2,i} = V_{1,i} + \frac{1}{2}(\sigma_{2,i}^2 + \gamma_{1,i}\tilde{\theta}_{1,i}^2 + \gamma_{2,i}\tilde{\theta}_{2,i}^2 + \gamma_{3,i}\tilde{\theta}_{3,i}^2), \tag{37}$$

taking the derivative w.r.t time of (37), considering (35)-(36) and

$$\tilde{\theta}_i = \theta_i - \hat{\theta}_i \text{ and } \dot{\tilde{\theta}}_i = -\dot{\hat{\theta}}_i$$

due that the uncertain parts of the parameters are slow to change with respect to time, it results

$$\begin{aligned} \dot{V}_{2,i} &= \sigma_{1,i}\sigma_{2,i} - k_{1,i}\sigma_{1,i}^2 + \sigma_{2,i}[-(\hat{\theta}_{1,i} + \tilde{\theta}_{1,i})(x_{1,i} \\ &- x_{3,i}) - (\hat{\theta}_{2,i} + \tilde{\theta}_{2,i})(x_{2,i} - x_{4,i}) + (\hat{\theta}_{3,i} + \tilde{\theta}_{3,i})u_i \\ &+ k_{1,i}\dot{\sigma}_{1,i}] - \gamma_{1,i}\tilde{\theta}_{1,i}\dot{\hat{\theta}}_{1,i} - \gamma_{2,i}\tilde{\theta}_{2,i}\dot{\hat{\theta}}_{2,i} - \gamma_{3,i}\tilde{\theta}_{3,i}\dot{\hat{\theta}}_{3,i}. \end{aligned} \tag{38}$$

According to (38), the control law can be defined as

$$u_i = \frac{1}{\hat{\theta}_{3,i}}[\hat{\theta}_{1,i}x_{1,i} + \hat{\theta}_{2,i}x_{2,i} - \sigma_{1,i} - k_{1,i}\dot{\sigma}_1 - k_{2,i}\sigma_{2,i}] \tag{39}$$

and the function $\dot{V}_{2,i}$ yields

$$\begin{aligned}\dot{V}_{2,i} &= -k_{1,i}\sigma_{1,i}^2 - k_{2,i}\sigma_{2,i}^2 - \tilde{\theta}_{1,i}[\sigma_{2,i}x_{1,i} + \gamma_{1,i}\dot{\hat{\theta}}_{1,i}] \\ &- \tilde{\theta}_{2,i}[\sigma_{2,i}x_{2,i} + \gamma_{2,i}\dot{\hat{\theta}}_{2,i}] + \tilde{\theta}_{3,i}(\sigma_{2,i}u_i - \gamma_{3,i}\dot{\hat{\theta}}_{3,i}) \\ &+ \rho_i\sigma_{2,i}\end{aligned} \tag{40}$$

where $\rho_i = \theta_{1,i}x_{3,i} + \theta_{2,i}x_{4,i}$. The adaptive laws are

$$\begin{aligned}\dot{\hat{\theta}}_{1,i} &= -\frac{1}{\gamma_{1,i}}\sigma_{2,i}x_{1,i}, \quad \dot{\hat{\theta}}_{2,i} = -\frac{1}{\gamma_{2,i}}\sigma_{2,i}x_{2,i} \\ \dot{\hat{\theta}}_{3,i} &= \frac{1}{\gamma_{3,i}}\sigma_{2,i}u_i,\end{aligned} \tag{41}$$

hence

$$\begin{aligned}\dot{V}_{2,i} &= -k_{1,i}\sigma_{1,i}^2 - k_{2,i}\sigma_{2,i}^2 + \rho_i\sigma_{2,i} \\ &= -k_{1,i}\sigma_{1,i}^2 - k_{2,i}\sigma_{2,i}^2 + k_{2,i}\epsilon_{1,i}\sigma_{2,i}^2 \\ &- k_{2,i}\epsilon_{1,i}\sigma_{2,i}^2 + \rho_i\sigma_{2,i} \\ &= -k_{1,i}\sigma_{1,i}^2 - \sigma_{2,i}^2k_{2,i}(1-\epsilon_{1,i}) \\ &- k_{2,i}\epsilon_{1,i}\sigma_{2,i}^2 + \rho_i\sigma_{2,i} \\ &\leq -k_{1,i}\sigma_{1,i}^2 - \sigma_{2,i}^2k_{2,i}(1-\epsilon_{1,i}),\end{aligned} \tag{42}$$

with $k_{1,i} > 0, k_{2,i} > 0$, $0 < \epsilon_{1,i} < 1$ and $\forall\ |\sigma_{2,i}| \geq \frac{|\rho_i|}{k_{2,i}\epsilon_{1,i}}$ [9] where $|\rho_i|$ is explained in detail in the Appendix.

IV. Simulations

This section shows the simulation results of the proposed SM control algorithms and the ABC. Vehicle and suspension parameters used in simulation are: $M_s = 1500$ kg, $m_{s,i} = 375$ kg, $m_{u,i} = 59$ kg, $I_x = 460$ Kg m^2, $I_y = 2160$ Kg m^2, $K_{FR} = K_{FL} = 35000$ Kg m^2, $K_{RR} = K_{RL} = 38000$ Kgm^2, $K_{t,i} = 1900000$ Kg m^2, $B_{FR} = B_{FL} = 1000$ Ns/m, $B_{RR} = B_{RL} = 1100$ Ns/m, $B_{t,i} = 170$ Ns/m $a = 1.4$ m, $b = 1.7$ m, $d = 0.45$ m. Figure 2 shows the road disturbances for both front and rear tires. The simulation routine is that during driving, the front tires are the first to be disturbed at $1 \leq t \leq 2$ s and the rear tires later at $1.5 \leq t \leq 2.5$ s. For this reason, and according to this perturbation, the roll dynamics will not be shown in the simulations because it is not affected. For comparison purpose, the response of the vehicle in open-loop to these disturbances is shown. After that, the behavior of the vehicle with quasi-continuous, nested and ST sliding mode controllers and ABC are presented, respectively. Please note that only positions of sprung mass and unsprung mass of the left side of the vehicle $x_{1,rl}$, $x_{1,fl}$, $x_{3,rl}$ and $x_{3,fl}$ are depicted as these signals are almost identical to those on the right side.

A. Open-Loop

The behavior of both the vertical position of the sprung mass and the unsprung mass of each tire are shown in Figure 3. It can be noted the oscillatory movement of both masses subject to the road disturbance. This open-loop response

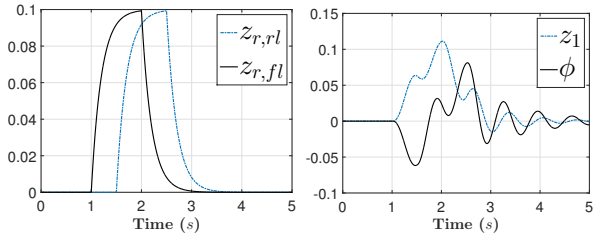

Fig. 2. Left: Road disturbances (meters). Right: sprung mass position at center of gravity (meters) and pitch angle (rad). Open-loop.

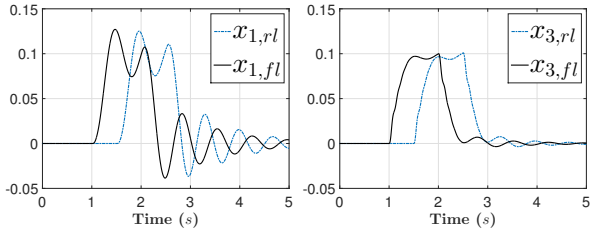

Fig. 3. Sprung mass vertical position and unsprung mass vertical position for each tire (meters). Open-loop.

produces discomfort of the passengers and possibly the vehicle instability.

Figure 2 shows the vertical position of the sprung mass and the pitch angle with respect to the center of gravity of the vehicle. It is important to mention that the behavior of these variables directly impacts on the movements that the vehicle presents and the passengers perceive. According to this figure, the passengers will experience an oscillatory movement produced by the road disturbance.

B. Nested Second-Order SM controller

For the nested second-order SMC, the four sliding functions were designed as $\sigma_i = x_{1,i}$. For the second-order robust exact differentiator, the parameters used in simulations were: $L = 1000$, $\lambda_0 = 1.1$; $\lambda_1 = 2.4$ and $\lambda_2 = 2$. The control gains were set to $\alpha_{1,i} = \alpha_{2,i} = 4,000$. Figure 4 shows the sprung mass displacement and the unsprung mass vertical position for each tire. As it can be seen, the effect of the road disturbance was widely reduced w.r.t. the open-loop behavior and it is despicable for the sprung mass, since the unsprung mass absorbs almost the complete disturbance. However, the produced chattering effect was considerable.

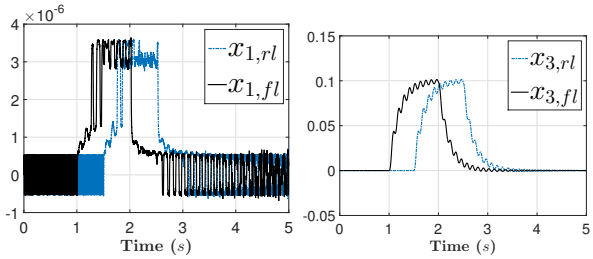

Fig. 4. Sprung mass vertical position and unsprung mass vertical position for each tire (meters): nested SM controller.

Figure 5 shows the sprung mass position and the pitch

angle at center of gravity. It is appreciated that both movements remains in a small boundedness, which ensures the passengers comfortableness. The control inputs responses of

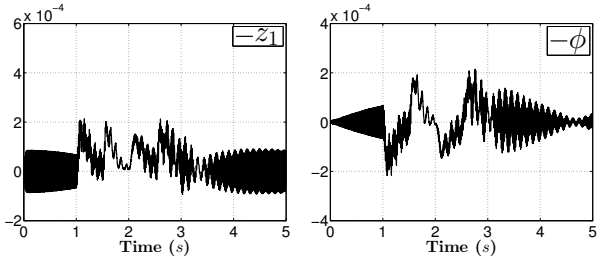

Fig. 5. Left: sprung mass position at center of gravity (meters). Right: pitch angle (rad). Nested SM controller.

the vehicle are shown in Figure 6. Only control signals of the left side of the vehicle (u_{rl} and u_{fl}) are depicted, as the control signals of the right side are almost identical.

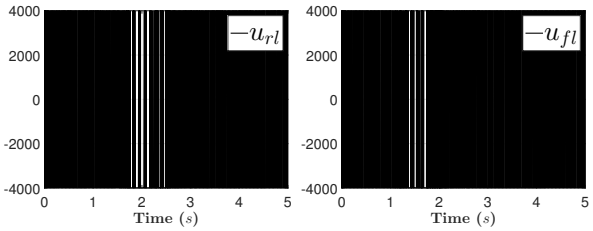

Fig. 6. Control inputs for each tire (N): nested SM controller.

C. Quasi-continuous SM controller

In this case, the same sliding surfaces, control gains and values for the differentiator coefficients of the nested controller were used. According to Figures 7-8, it can be noticed that the behavior of the closed-loop system with this controller is very similar to that obtained using the nested controller. However, the transient response peak at the sprung mass displacements result smaller.

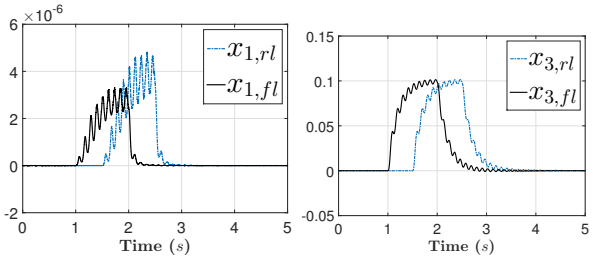

Fig. 7. Sprung mass vertical position and unsprung mass vertical position for each tire (meters): quasi-continuous SM controller.

A difference in the applied control input w.r.t. the nested controller can be seen in Figure 9, where the quasi-continuous control law produces, approximately between 1.5 and 2.5 seconds, a decreasing in the control abrupt changes.

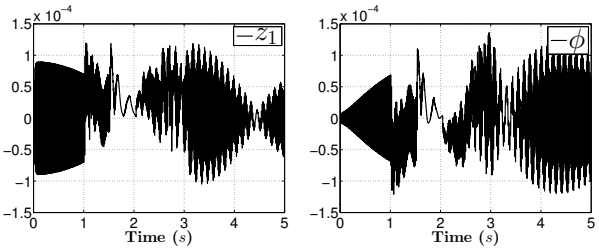

Fig. 8. Left: sprung mass position at center of gravity (meters). Right: pitch angle (rad). Quasi-continuous SM controller.

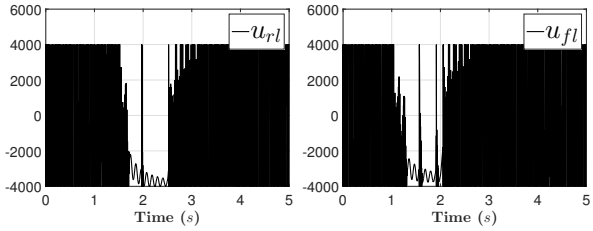

Fig. 9. Control inputs for each tire (N): quasi-continuous controller.

D. Super-Twisting controller

For the ST controller, the four sliding functions were designed as $\sigma_i = 10x_{1,i} + x_{2,i}$, while the ST gains were set to $k_{1,i} = k_{2,i} = 10,000$. Figure 10 shows the sprung mass displacement and the unsprung mass vertical position for each tire. The ST controller shows a good performance in the displacement magnitude and, in addition, the transient response for this control algorithm was dramatically improved, obtaining just a few oscillations. The unsprung mass vertical position almost counteract the disturbance effect, achieving that the sprung mass stay in a small boundedness of the equilibrium point.

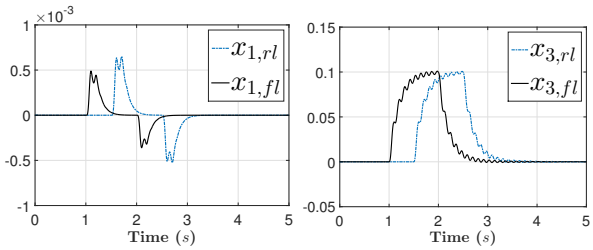

Fig. 10. Sprung mass vertical position and unsprung mass vertical position for each tire (meters): super-twisting controller.

Figure 11 shows the resulting sprung mass displacement and pitch angle at the car center of gravity and the corresponding control inputs. It can be seen that, unlike the previous controllers, the continuous nature of the ST algorithm produces a smoother response of the control input, achieving an important chattering reduction in the system responses.

E. Adaptive backstepping controller

For the ABC, the control gains were set to $k_{1,i} = 25$ and $k_{2,i} = 1000$ and the adaptive gains were set to $\gamma_{1,i} = 0.1$,

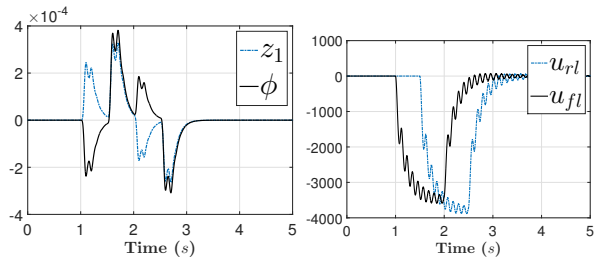

Fig. 11. Left: sprung mass position at center of gravity (meters) and pitch angle (rad). Right: Control inputs for each tire (N). Super-twisting controller.

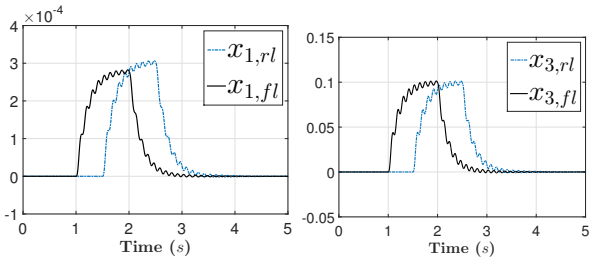

Fig. 12. Sprung mass vertical position and unsprung mass vertical position for each tire (meters): adaptive backstepping controller.

$\gamma_{2,i} = 0.1$ and $\gamma_{3,i} = 100000000$. Figure 12 shows the sprung mass displacement and the unsprung mass vertical position for each tire. The ABC shows a very simulated behavior compared to the performance of the ST controller. Figure 13 shows the resulting sprung mass displacement and

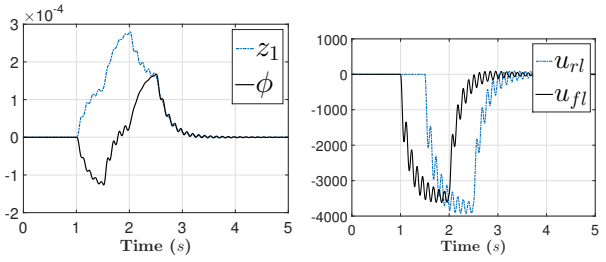

Fig. 13. Left: sprung mass position at center of gravity (meters) and pitch angle (rad). Right: Control inputs for each tire (N). Adaptive backstepping controller.

pitch angle at the car center of gravity and it shows control inputs, which also resemble the control inputs of the ST algorithm.

V. Conclusions and Future Work

The stabilization of the vertical position, pitch and roll motions of a car with active suspension was successfully addressed using three different HOSM algorithms. The first two proposed controllers, quasi-continuous and nested SM, showed a similar satisfactory performance as both keeps the car vertical displacement in a small vicinity of zero, despite the disturbances. On the other hand, the ST and adaptive backstepping controllers achieved a superior performance by, additionally, showed a smoother transient response and control signals. Future works will consider a more extensive car model, combining the suspension dynamics presented in this paper with longitudinal, lateral, yaw and roll dynamics.

Appendix

The bound of disturbance term that appears in the adaptive backstepping controller, $|\rho_i|$ can be founded following the next steps:

1 Due that the parameters to adaptive $\theta_{1,i}$, $\theta_{2,i}$ and $\theta_{3,i}$ from

$$\rho_i = \theta_{1,i} x_{3,i} + \theta_{2,i} x_4 \tag{43}$$

are values that correspond to physical elements, these have a finite value, i.e., they can be bounded by

$$1 \leq \theta_{1,i} \leq \beta_{1,i} \quad \text{and} \quad 1 \leq \theta_{2,i} \leq \beta_{2,i}. \tag{44}$$

2 In addition, x_3 and x_4 must be bounded, for this we analyze this as the zero dynamics of the system. Considering $x_{1,i} = x_{2,i} = 0$ and $u_i = 0$, from (6), it is obtained that

$$\begin{aligned} \dot{x}_{3,i} &= x_{4,i} \\ \dot{x}_{4,i} &= -\frac{(K_i + K_{t,i})}{m_{u,i}} x_{3,i} - \frac{(B_i + B_{t,i})}{m_{u,i}} x_{4,i} \\ &+ \frac{K_{t,i}}{m_{u,i}} z_{r,i} + \frac{B_{t,i}}{m_{u,i}} \dot{z}_{r,i}. \end{aligned} \tag{45}$$

The terms $\frac{(K_i + K_{t,i})}{m_{u,i}} > 0$ and $\frac{(B_i + B_{t,i})}{m_{u,i}} > 0$ due they correspond to physical elements. Hence, it can be seen that system (45) is stable since

$$\begin{bmatrix} 0 & 1 \\ -\frac{(K_i + K_{t,i})}{m_{u,i}} & -\frac{(B_i + B_{t,i})}{m_{u,i}} \end{bmatrix}$$

is Hurwitz and $|z_r| \leq \vartheta_{1,i}$ and $|\dot{z}_r| \leq \vartheta_{2,i}$, where $\vartheta_{1,i}$ and $\vartheta_{2,i}$ are nonnegative constants.

3 According with the last, $\rho_{1,i}$ can be bounded as

$$|\rho_i| \leq \beta_{1,i} x_{3,i} + \beta_{2,i} x_{4,i} \leq \mu_i, \tag{46}$$

where μ_i is a positive constant.

References

[1] Z. Lou, R. Ervin, and F. Filisko, "A preliminary parametric study of electrorheological dampers," *Journal of fluids engineering*, vol. 116, no. 3, pp. 570–576, 1994.

[2] W. Sun, H. Gao, and O. Kaynak, "Finite frequency control for vehicle active suspension systems," *IEEE Transactions on Control Systems Technology*, vol. 19, no. 2, pp. 416–422, 2011.

[3] J.-S. Lin and C.-J. Huang, "Nonlinear backstepping control design of half-car active suspension systems," *International Journal of Vehicle Design*, vol. 33, no. 4, pp. 332–350, 2003.

[4] C. Kim and P. I. Ro, "An accurate full car ride model using model reducing techniques," *Journal of mechanical design*, vol. 124, no. 4, pp. 697–705, 2002.

[5] A. Levant, *Homogeneous Quasi-Continuous Sliding Mode Control*. Berlin, Heidelberg: Springer Berlin Heidelberg, 2006, pp. 143–168.

[6] L. Fridman and A. Levant, *Sliding Mode Control in Engineering*. New York: Marcel Dekker, 2002, ch. Higher order sliding modes, pp. 53–102.

[7] J. A. Moreno and M. Osorio, "A Lyapunov approach to second-order sliding mode controllers and observers," in *Decision and Control, 2008. CDC 2008. 47th IEEE Conference on*. IEEE, 2008, pp. 2856–2861.

[8] M. Krstic, I. Kanellakopoulos, and P. V. Kokotovic, *Nonlinear and adaptive control design*. Wiley, 1995.

[9] H. K. Khalil and J. Grizzle, "Nonlinear systems, vol. 3," *Prentice hall Upper Saddle River*, 2002.